Internal Dynamics of Human Ubiquitin Revealed by ^{13}C-Relaxation Studies of Randomly Fractionally Labeled Protein[†]

A. Joshua Wand,* Jeffrey L. Urbauer, Robert P. McEvoy,[‡] and Ramona J. Bieber

Department of Chemistry and Center for Structural Biology, State University of New York at Buffalo, Buffalo, New York 14260

Received December 20, 1995; Revised Manuscript Received February 28, 1996[⊗]

ABSTRACT: The use of random, fractional ^{13}C-enrichment combined with low pass filtration has allowed the determination of NMR relaxation parameters at an unprecedented number of sites within recombinant human ubiquitin. Essentially complete ^{1}H, ^{13}C, and ^{15}N resonance assignments for the protein are reported. Carbon spin lattice and heteronuclear NOE relaxation data have been analyzed in the context of the Lipari−Szabo "model free" formalism. The generalized order parameters for 56 main chain α C−H vectors have been determined and are found to correspond to the highly restricted motion seen in previous studies of the motion of amide N−H vectors. In distinct contrast, the analysis presented here indicates an unexpected range of dynamics within the interior of the protein. The generalized order parameters of 45 methyl groups of human ubiquitin have been determined. The methyl groups of Thr and Ala residues show generalized order parameters ranging from the Woessner limit (0.111) to below 0.01. Generalized order parameters for all methyl groups of the seven isoleucine residues were determined. With one exception, the generalized order parameters of the γ methyls were equal to or greater than the corresponding δ methyls, indicating higher mobility away from the main chain. Generalized order parameters for 11 methyl groups of leucine residues were also determined. In six of the seven cases where the generalized order parameters of both prochiral methyl groups were determined, the *pro-R* methyl consistently shows a higher value than the *pro-S* methyl group. Generalized order parameters for seven methyl groups of four valines were also determined. There is no apparent correlation of methyl group prochirality with the value of the generalized order parameter. These data have several implications and generally indicate that the interior of the protein is heterogeneously dynamic.

The physical basis of protein structure, dynamics, and stability has been a subject of intense study and debate for several decades. While our knowledge of the taxonomy of protein structure appears to be nearing completeness, an understanding of the existence, character, and interconversion of states near the lowest free energy state of proteins remains largely incomplete. These issues are fundamental to a complete understanding of the origins, temporal behavior, and marginal stability of protein structure. For example, empirical evidence indicates that entropic effects dominate the free energy changes that accompany folding of a solvated "random coil" polypeptide usually to a dominant structure of lower free energy. The observed net increase in system entropy upon folding has been attributed to the dominance of a large increase in solvent entropy upon side chain dehydration over a putatively smaller decrease in side chain entropy upon packing in the folded globular state. Atomic scale structural analysis of proteins has shown that proteins generally have extremely high packing densities, which in turn suggests that proteins are rigid with residual motion being extremely restricted and local. Acccordingly, in discussions of protein stability and related issues, it is commonly assumed that the residual entropy of proteins is negligible. Nevertheless, over the past two decades there has been an accumulation of experimental evidence that suggests quite a different view—that proteins are quite dynamic on time scales relevant to the question of residual entropy (Karplus et al., 1987). The magnitude of the residual entropy of proteins is of critical importance to an understanding of protein structure, stability, and ultimately function. In principle, nuclear magnetic resonance (NMR)[1] spectroscopy can be employed to estimate the local dynamics throughout a protein. However, though comprehensively applied to small polypeptides, the application of NMR relaxation techniques to the study of fast local dynamics throughout a protein has been hindered by the apparent need to employ selective ^{13}C-enrichment. Thus, although a number of studies of the motion of N−H vectors in proteins have been reported, there have been a paucity of reports on the internal dynamics of side chain C−H vectors of proteins. Here we apply a recently introduced technique to obtain reliable ^{13}C relaxation parameters in the protein ubiquitin. Ubiquitin is a small (76 amino acids) extremely stable protein containing a broad collection of secondary structure elements, including parallel and antiparallel β strands assembled into

[†] Supported by NIH Research Grants GM-35940 and DK-39806. This study made use of the National Nuclear Magnetic Resonance Facility at Madison which is supported by NIH Grant RR02301 from the Biomedical Research Technology Program, National Center for Research Resources. Equipment at the facility was purchased with funds from the University of Wisconsin, the NFS Biological Instrumentation Program (DMB-8415048), NSF Academic Research Instrumentation Program (BIR-9214394), NIH Biomedical Research Technology Program (RR02301), NIH Shared Instrumentation Program (RR02781 and RR08438), and the U.S. Department of Agriculture.

* To whom correspondence should be addressed.

[‡] Deceased.

[⊗] Abstract published in *Advance ACS Abstracts,* May 1, 1996.

[1] Abbreviations: NMR, nuclear magnetic resonance; NOE, nuclear Overhauser effect; pH*, pH meter reading uncorrected for the isotope effect; S^2, model free generalized order parameter; T_1, spin lattice relaxation time constant; τ_e, model free effective correlation time; τ_m, global isotropic tumbling time.

S0006-2960(95)03014-5 CCC: $12.00

a mixed β sheet, α and 3_{10} helices, and a variety of turns (Vijay-Kumar et al., 1987; Di Stefano & Wand, 1987). In previous work, we have examined the fast main chain dynamics of ubiquitin by use of NMR relaxation methods (Schneider et al., 1992). These data were analyzed in terms of the so-called model free treatment of Lipari and Szabo (1982a,b). The amplitudes of motion of the backbone amide N−H vectors of the packed regions of the protein are generally highly restricted and show no apparent correlation with secondary structure context but do show a strong correlation with the presence of hydrogen bonding of the amide hydrogen or its peptide bond associated carbonyl. These data suggest that the main chain of ubiquitin has highly restricted motion on the subnanosecond time scale and that molecular packing interactions provide the dominant restriction to this motion. Although informative, the study of ^{15}N relaxation in ubiquitin failed to provide any insight as to the extent, range, and character of side chain dynamics. To obtain a measure of the amplitude and timescale of fast (subnanosecond) dynamics of C−H vectors of both the main chain and side chains, we have carried out low pass filtered NMR relaxation experiments using 15% randomly ^{13}C-enriched ubiquitin. Analysis of the relaxation parameters of methine carbon and methyl carbon centers reveals a wide range of side chain dynamics throughout the interior of the protein. In contrast to these results, but in general agreement with the view of the main chain provide by amide N−H dynamics, the relaxation behavior of α carbon sites is consistently indicative of low amplitude−high frequency motion along the backbone of the protein.

MATERIALS AND METHODS

Preparation of ^{13}C-Enriched Ubiquitin. The ubiquitin structural gene construct was synthesized as described by Ecker et al. (1987a) with minor modifications which included the deletion of the 5′ *Nde*I restriction site and the addition of an *Xba*I restriction site, a ribosome binding site, a start codon, and an additional stop codon. The gene was assembled from four oligonucleotides each separately cloned into the pBluescript II SK (+/−) plasmid (Stratagene) and sequenced using standard protocols (Sambrook et al., 1989). Within the structural gene, an *Xba*I site was removed and an *Eco*R I site added to facilitate further manipulation. The complete gene was assembled by ligation and sequenced. To facilitate cloning of the ubiquitin gene into a pET series expression vector, *Bam*HI and *Kpn*I restriction sites were added directly preceding the *Nco*I restriction site in the pET-15b vector (Novagen). The ubiquitin gene construct described above was ligated into the modified pET-15b vector and used to transform *Escherichia coli* strain BL21(DE3). Expression was undertaken in minimal media containing M9 salts and the desired nitrogen and carbon source. Three types of ubiquitin samples were prepared. Uniformly ^{15}N,^{13}C-labeled ubiquitin was prepared utilizing [$^{13}C_6$]-glucose (2 g/L) and $^{15}NH_4Cl$ (1 g/L). The sample used for relaxation studies was prepared using a mixture of acetates (4 g/L) comprised of 15% [$^{13}C_1$]acetate, 15% [$^{13}C_2$]acetate, and 70% unlabeled acetate. To determine prochiral methyl assignments, ubiquitin was prepared using a mixture of uniformly ^{13}C-labeled glucose (10%) and unlabeled glucose (90%). Ubiquitin was purified by a minor variation of the standard protocol (Ecker et al., 1987b). NMR samples ranged between 2 and 4 mM in ubiquitin and were prepared in 50 mM potassium phosphate buffer, pH* 5.7, in 90% H_2O and 10% D_2O or 100% D_2O as required.

NMR Spectroscopy. Spectra were recorded on Bruker AMX-500 and DMX-750 NMR spectrometers at 30 °C. All triple resonance experiments and the HCCH-TOCSY experiment were performed on a single sample of [^{15}N,^{13}C]ubiquitin in 90% H_2O/10% D_2O buffer. HCCH-TOCSY spectra were obtained using the pulse sequence described by Bax et al. (1990) and utilized a 27 ms DIPSI-3 mixing sequence. The HCCH-TOCSY data sets were composed of 92 complex points in the incremented ^{1}H dimension, 48 complex points in the incremented ^{13}C dimension, and 256 complex points in the ^{1}H acquisition dimension. The obtained data sets were transformed to 256 by 128 by 512 points for the ^{1}H, ^{13}C, and ^{1}H dimensions spanning 4000, 4310, and 4000 Hz, respectively. HNCA, HNCO, and HN(CO)CA experiments were obtained essentially as described by Grzesiek and Bax (1992) and were composed of 52 (HNCA and HN(CO)CA) or 64 (HNCO) complex points in the incremented ^{13}C dimension, 32 complex points in the incremented ^{15}N dimension, and 512 complex points in the ^{1}H acquisition dimension. The obtained data sets were transformed to 128 (HN(CO)CA and HNCA) or 256 (HNCO) by 128 by 512 points for the ^{13}C, ^{15}N, and ^{1}H dimensions spanning 3333, 2016, and 6410 Hz, respectively. Constant time ^{13}C−HSQC spectra were collected as described by Vuister and Bax (1992). The ^{13}C−HSQC spectrum without ^{13}C-decoupling during the incremented time domain was acquired as described by Neri et al. (1990). NOE and spin lattice relaxation were monitored using the pulse sequences described in Figure 1. A 3 s period of composite pulse ^{1}H decoupling was used to generate the steady-state NOE. All data processing was done using the program FELIX (Biosym Technologies). Spectra are referenced to trace TMS in water (^{1}H, 0 ppm), neat TMS (^{13}C, 2.86 ppm), and $^{15}NH_4Cl$ in 1 M HCl (^{15}N, 24.93 ppm).

Relaxation Data Analysis. Center cross peak intensities of the serial two-dimensional ^{13}C−HSQC spectra used to quantitate spin lattice relaxation were fitted to a two parameter single exponential using standard Gaussian elimination methods. The heteronuclear NOE was determined using cross peaks of ^{13}C−^{1}H correlation spectra obtained with and without saturation of proton resonances which were integrated and corrected for baseline offsets as required. Model free order parameters were obtained using eqs 1−3 and 5 as described in the text and by Dellwo and Wand (1989). Estimates of the error in the obtained model free parameters were obtained from the variation of the model free parameters during Monte Carlo sampling of the observed relaxation parameters over the range of their estimated individual precision.

RESULTS AND DISCUSSION

^{13}C-Resonance Assignments. The essentially complete assignment of ^{1}H, ^{13}C, and ^{15}N resonances of recombinant human ubiquitin were obtained by analysis of HNCA, HN(CO)CA, HNCO, and HCCH-TOCSY spectra and reference to previously reported ^{1}H (Di Stefano & Wand, 1987) and ^{15}N (Schneider et al., 1992) resonance assignments. Main chain ^{13}C and ^{15}N haven been recently reported (Wang et al., 1995) and are consistent with our correction of two previous ^{15}N resonance assignments. Of primary interest

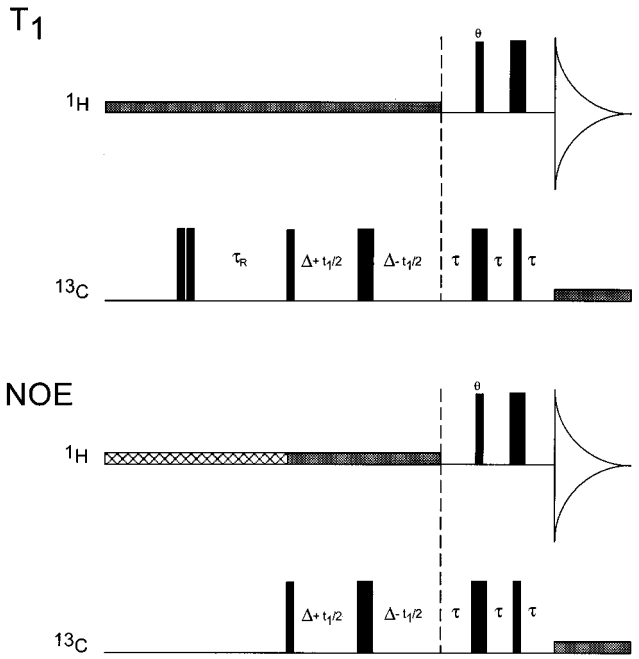

FIGURE 1: Pulse sequences used to monitor the heteronuclear NOE (lower panel) and the spin lattice relaxation (upper panel). The NOE experiment is a simple extension of the basic pulse sequence introduced by Kay et al. (1989) and utilizes continuous broadband ^{1}H decoupling during the preparation period to generate the NOE. Two dimensional spectra with and without ^{1}H decoupling (hatched region) define the NOE. In the upper panel, the T_1 relaxation experiment is a simple extension of the basic pulse sequence introduced by Sklenar et al. (1987). The NOE via ^{1}H decoupling rather than coherent polarization transfer is used to polarize the carbons. For both the NOE and T_1 measurement, the proton pulse θ (or the delay of the corresponding reverse INEPT) is set to the magic angle as described by Palmer et al. (1991). The constant time period, D, is set to minimize $\cos[(n)(2\pi\tau^1J_{CC} + 2\pi\Delta^1J_{CH})]$. When t is set to $1/2J_{CH}$ then $2\Delta = 1/2^1J_{CC} - 1/^1J_{CH}$, resulting in the suppression of the contribution of ^{13}C−^{13}C−^{1}H spin systems to the observed relaxation (see Wand et al., 1995). The value of n allows a null to be obtained at different constant time intervals, providing for increased digital resolution at the expense of sensitivity.

here are the α carbon and side chain methyl carbon resonance assignments. HCCH-TOCSY spectra provided unequivocal correlations for the majority of carbon resonances of ubiquitin. Examples are shown in Figure 2. Stereospecific assignments of leucine δ-CH_3 and valine γ-CH_3 groups were obtained using the isotopic labeling strategy developed by Neri et al. (1989, 1990). This approach provided unequivocal prochiral assignments for all of the valine and leucine methyl pairs. The essentially complete ^{1}H, ^{15}N, and ^{13}C resonance assignments of recombinant human ubiquitin are listed in the Supporting Information.

Determination of T_1 and NOE Relaxation Parameters. Human ubiquitin was randomly and fractionally enriched with ^{13}C by expression of the protein in *E. Coli* during growth on mimimal media utilizing a mixture of labeled and unlabeled acetates (15% [$^{13}C_2$]acetate, 15% [$^{13}C_1$]acetate, 70% [$^{12}C_1$,$^{12}C_2$]acetate) as the sole carbon source. Low pass filtered indirectly detected T_1 relaxation experiments were utilized to suppress contributions from ^{13}C−^{13}C pairs to the constant time HSQC spectra used to sample relaxation (Wand et al., 1995; see Figure 1). To simplify analysis of heteronuclear relaxation, obtained relaxation parameters must be overwhelmingly dominated by ^{1}H−^{13}C dipolar interactions. In randomly fractionally ^{13}C-enriched protein there

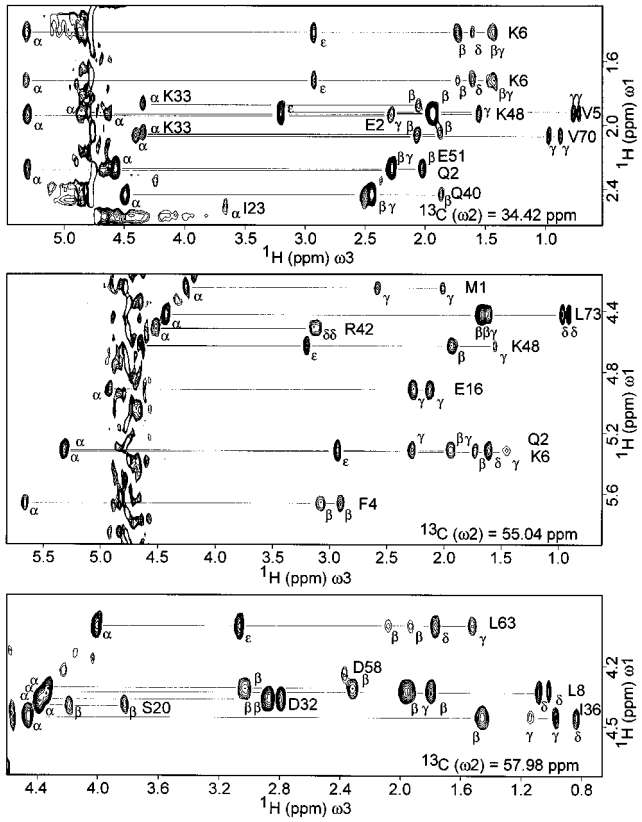

FIGURE 2: Expansions of a three-dimensional HCCH-TOCSY spectrum of [^{15}N,^{13}C]ubiquitin in 90% H_2O/10% D_2O, 50 mM potassium phosphate buffer, pH* 5.7 at 30 °C. Resonance assignments were aided by comparison to previously reported main chain ^{1}H and ^{15}N (Schneider et al., 1992) and side chain ^{1}H assignments (Di Stefano & Wand, 1987).

will be a population of ^{13}C nuclei bonded to other ^{13}C nuclei. The contributions of this subpopulation to the obtained two-dimensionally sampled relaxation profile is suppressed by low pass filtration based on ^{13}C−^{13}C scalar coupling (Wand et al., 1995). The pulse sequence used to sample T_1 relaxation polarizes the ^{13}C nuclei via the NOE, utilizes a difference T_1 time course, and increases sensitivity by use of a reverse DEPT (or INEPT) sequence. This approach has several distinct advantages over the double DEPT sequences used to study methine carbon or amide nitrogen relaxation. Simple polarization with the NOE avoids creation of unwanted and complicating multiple spin coherences and allows use of ^{1}H decoupling throughout the low pass filter with similar advantages. Complications with individual multiplet component transfer and relaxation through the constant time evolution and filter are also avoided.

T_1 relaxation obtained at 17.6 T was sampled at 0.01, 0.16, 0.31, 0.46, 0.61, 0.76, 0.91, 1.06, 1.21, 1.36, 1.51, and 1.66 s following inversion. T_1 relaxation obtained at 11.3 T was sampled at 0.01, 0.11, 0.21, 0.31, 0.41, 0.51, 0.61, 0.71, 0.81, 0.91, 1.01, and 1.11 s following inversion. In all cases, a constant time period of 36 ms was used which corresponds to a predicted null in the intensity contributed by ^{13}C−^{13}C−^{1}H spin systems. The obtained relaxation curves were uniformly singly exponential for both methine and methyl carbon sites. Examples are shown in Figure 3. Methyl group ^{13}C T_1 relaxation profiles were essentially insensitve to the value of the low pass filter delay used. This is consistent with the small fraction (15%) of ^{13}C nuclei bonded to [^{13}C]-methyl carbons in the preparation of randomly fractionally

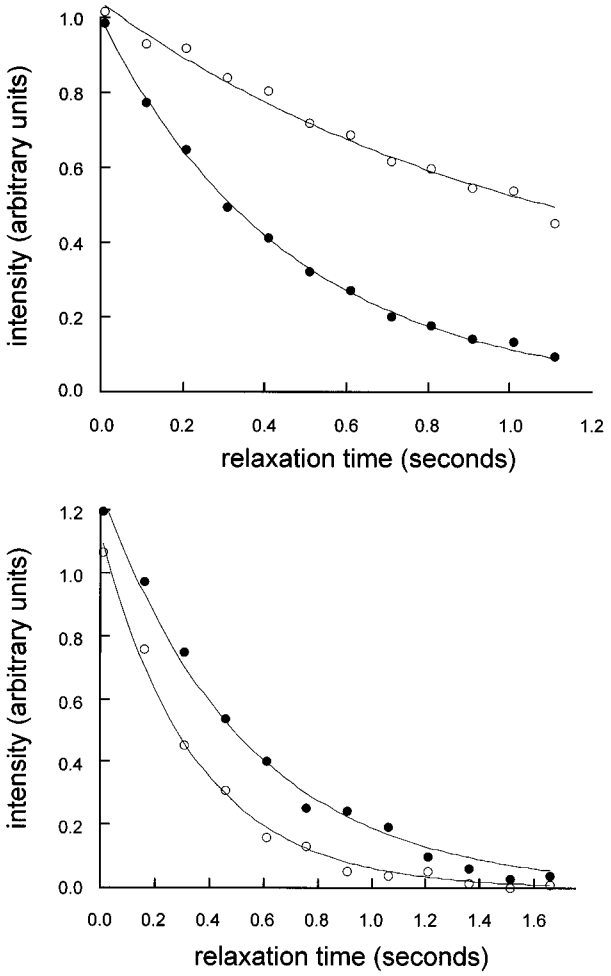

FIGURE 3: Examples of spin lattice relaxation curves obtained at 17.6 T using 4 mM 15% randomly fractionally ^{13}C-enriched ubiquitin. Peak maxima of the designated ^{13}C−^{1}H correlation cross peak are plotted as a function of the relaxation time period.

^{13}C-enriched ubquitin used. Obtained T_1 relaxation profiles of methine carbons, having potentially up to three adjacent carbon sites, showed some sensitivity to variation of the low pass filter delay from the null value to nonoptimal values.

Extensive decoupling during relaxation, appropriate setting of the proton pulse of the reverse DEPT (or the delays of the reverse INEPT) to the magic angle, and use of incoherent polarization give a decidedly single exponential character to the T_1 relaxation data. This indicates the absence of significant cross-correlation and other potentially contaminating effects (Werbelow & Grant, 1977), as extensively discussed in this context by Palmer et al. (1991) and Kay et al. (1992). Indeed, the simulations of the effects of dipolar cross correlation on methyl carbon T_1 and NOE parameters predict only a small effect for the global and internal correlation times seen in this study (Kay & Torchia, 1991). One expects, then, that the data obtained accurately represent the T_1 and NOE relaxation parameters that would be obtained in a standard direct detection experiment.

The constant time period, required to suppress contamination by ^{13}C−^{13}C−^{1}H spin systems, places a restriction on the digital resolution in the ^{13}C chemical shift dimension of the obtained HSQC spectra. Using a constant time period of 36 ms, the extensively folded ^{13}C−HSQC spectrum allowed spin lattice relaxation at a total of 56 α carbon and 45 methyl carbon sites to be adequately quantitated.

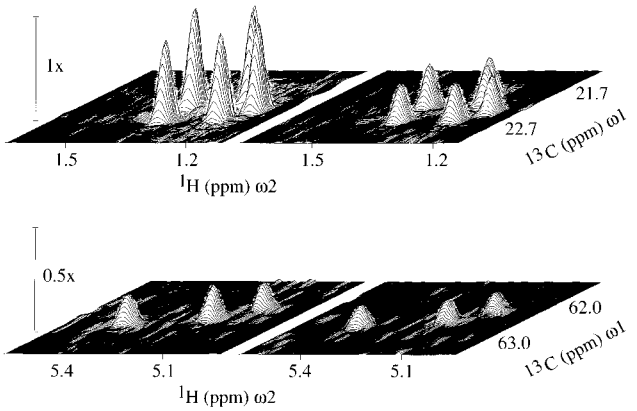

FIGURE 4: Examples of cross peak intensities obtained with and without preparation with the NOE. Shown are stacked plots of expansions of the ^{13}C−HSQC spectrum used to sample intensities of methyl carbons with (top left) and without (top right) the NOE. The intensity of several α methine carbon resonances with (bottom left) and without (bottom right) the NOE are also shown. The spectra were obtained at 11.3 T.

Statistical analysis of the fitted T_1 relaxation curves and their reproducibility ($n = 3$) indicate that with few exceptions the precision of obtained spin lattice relaxation rates is better than 3%. There is no significant systematic difference in precision of relaxation rates obtained at 11.3 or 17.6 T. NOE values obtained were slightly less precise, averaging better than 5% using the criteria of Nicholson et al. (1992). The quality of the NOE data is indicated by the stacked plot expansions shown in Figure 4. For a small number of α carbon sites, the obtained heteronuclear NOE is slightly less than the minimum value (1.17) expected for a rigid vector tumbling isotropically with the 4.125 ns correlation time previously determined for ubiquitin (Schneider et al., 1992). We attribute this to experimental error for data obtained at otherwise internally rigid centers.

Interpretation of T_1 and NOE Relaxation Parameters. The T_1 and NOE relaxation parameters for a ^{13}C spin relaxed solely by dipole−dipole interactions with a directly bonded proton spin are given by (Wittebort & Szabo, 1978):

$$\frac{1}{T_1} = \frac{\hbar^2 \gamma_H^2 \gamma_C^2}{4 r_{CH}^6}[J(\omega_H - \omega_C) + 3J(\omega_C) + 6J(\omega_H + \omega_C)] \quad (1)$$

$$\mathrm{NOE} = 1 + \frac{\gamma_H[6J(\omega_H + \omega_C) - J(\omega_H - \omega_C)]}{\gamma_C[J(\omega_H - \omega_C) + 3J(\omega_C) + 6J(\omega_H + \omega_C)]} \quad (2)$$

where γ_H, γ_C, $\hbar$, and r_{CH} correspond to the gyromagnetic ratios characteristic of hydrogen and carbon, Planck's constant, and the C−H bond length, respectively. The effects of other relaxation mechanisms such as chemical shift anisotropy (Spiess, 1978) and spin rotation (Spiess et al., 1973) can be assumed to be negligible for methyl groups. The CSA of α and side chain methines such as the β-carbon of threonine may be as large as 20−40 ppm but are also not expected to contribute significantly to the relaxation rate determined.

Given knowledge of the covalent geometry and fundamental constants underlying relaxation, the spectral densities, $J(\omega)$, remain to be defined. Here, we adopt the so-called model free treatment due to Lipari and Szabo

(1982a,b) which seeks to encapsulate the unique motional character expressed in observed relaxation behavior by defining the spectral density in terms of two local parameters:

$$J(\omega) = \frac{2}{5}\left[\frac{S^2\tau_m}{1+\omega^2\tau_m{}^2} + \frac{(1-S^2)\tau}{1+\omega^2\tau^2}\right] \quad (3)$$

where $1/\tau = 1/\tau_e + 1/\tau_m$ and S^2, τ_m, and τ_e correspond to the generalized order parameter, the global isotropic tumbling correlation time, and the effective internal correlation time, respectively. S^2 reflects the spatial restriction of the internal motion and is defined as:

$$S^2 = \sum_{m=-2}^{2}\left|\left\langle \frac{C_{2m}(\Omega)}{r_{CH}{}^3}\right\rangle\right|^2 \quad (4)$$

where Ω corresponds to the polar angles of the C−H vector in a frame of reference rigidly attached to the molecule (Lipari & Szabo, 1982a,b). When S^2 is 1, the motion at that site is completely restricted internally. In the limit of completely unrestricted (isotropic) internal motion, S^2 would equal zero although it should be noted that the converse is not necessarily true. The effective correlation time, τ_e, provides an upper limit on the time scale of the internal motion and is formally defined as the area of the internal correlation function. The global correlation time, τ_m, corresponds to isotropic global tumbling. It has been shown previously that, for relaxation data of the precision obtained herein, the internal dynamics of the protein are satisfactorily treated while employing an isotropic global tumbling model (Schneider et al., 1992). Recent work by Bax and co-workers has pointed to a very slight anisotropy to global tumbling which will not significantly affect the results obtained here (Tjandra et al., 1996).

The appropriateness the the model free treatment rests on its ability to successfully describe the internal correlation function describing internal motion by a single exponential (Lipari & Szabo, 1982a). Though the complexity of the motions undertaken by amino acid side chains may be quite complicated, the Padè approximation employed by the model free treatment would appear to provide a valid approach over a wide range of physically realistic motion (Lipari & Szabo, 1982a). In some cases, a significant separation of time scales of internal motions may result in a failure of the simplest form of the model free treatment, but this can usually be detected by poor fits of the primary relaxation data using eq 3 (see below and Clore et al., 1990).

Equation 3 indicates that two local model free parameters need to be determined for each site under investigation. Spin lattice relaxation rates obtained at two fields and the NOE obtained at one field were fitted to eqs 1 and 2, respectively, for an explicit range of values for S^2 and τ_e. Values of 1.1 Å for the C−H bond length and 4.125 ns (Schneider et al., 1992) for τ_m were used. The error function describing this fit is defined as (Dellwo & Wand, 1989):

$$\chi^2 = \sum_{\omega_1\ldots\omega_n}\left(\frac{T_1^{obs}-T_1^{calc}}{T_1^{obs}}\right)^2 + \left(\frac{NOE^{obs}/T_1^{obs} - NOE^{calc}/T_1^{calc}}{NOE^{obs}/T_1^{obs}}\right)^2 \quad (5)$$

For a perfect fit, the target function would equal zero. A fractional error was used to obtain equal weighting of the observed T_1 and NOE data. Spin−spin relaxation time constants (T_2) were not used owing to their sensitivity to motions occurring on much slower times scales. In principle, given completely accurate and precise observed relaxation data, one can use any combination of relaxation parameters to determine the underlying model free parameters. The presence of error can have significant influence on the values of obtained model free parameters, and it has been shown that the combined use of spin lattice relaxation times and nuclear Overhauser effects obtained at more than one field avoids systematic bias in obtained model free parameters (Dellwo & Wand, 1991).

Error grids of 500 values for S^2 ranging from 0 to 1 in 0.002 steps and 500 values of τ_e ranging from 0 to 1 ns in 2 ps steps were constructed for each site. Global minima were confirmed by visual inspection of the two-dimensional contour plots. Examples are shown in Figure 5. In general, normalized minima (χ^2/N) for all but a few sites were less than 5×10^{-3}, indicating that, on average, the simple model free spectral density function treated the experimental data to within its estimated precision.

Alpha C−H Dynamics. Generalized order parameters and effective correlation times for α C−H pairs were obtained for 56 residues (Table 1 and Figure 6). The order parameters range from essentially one (internally rigid) to approximately 0.3. However, the vast majority of generalized order parameters of backbone α C−H vectors in recombinant human ubiquitin are between 0.7 and 1.0. This is consistent with the view provided by backbone N−H dynamics that the main chain of the protein is relatively rigid (Schneider et al., 1992). There is no apparent simple distinction between different types of secondary structure (Figure 6). Most effective correlation times fall in the range between 50 and 500 ps (Table 1). Some residues show effective correlation times approaching or exceeding 1 ns, values which begin to violate the assumption underlying the model free treatment that $\tau_e \ll \tau_m$. The model free parameters obtained for these sites (e.g., I13, K48, S65) should therefore be interpreted with caution. In all cases determined, the effective correlation times of the α C−H vector of a given residue significantly exceeded that of the amide N−H vector of the same residue (see Schneider et al., 1992). For those residues found within an element of secondary structure, the α C−H S^2 is usually larger than the S^2 for the N−H of the same residue. In contrast, at the edge (in primary sequence) of an element of secondary structure, the α C−H S^2 is usually lower than those found within helix and sheet secondary structure elements and is usually smaller than the S^2 for the N−H of the same residue.

Methyl Group Dynamics. A simple model for the motion of a methyl group is the Woessner model, which predicts an order parameter based on the angle β between the C−H bond and the methyl group symmetry axis (Woessner, 1962). In this model, the reorientation occurs by either simple diffusion about the symmetry axis or by a jump−rotation mechanism interchanging the three equivalent sites. For perfect expected tetrahedral covalent geometry, where b equals 70.5°, a corresponding S^2 of 0.111 is obtained. Significant deviations of the generalized order parameter from this value indicate that the Woessner model is inappropriate. Values higher than 0.111 are inconsistent with

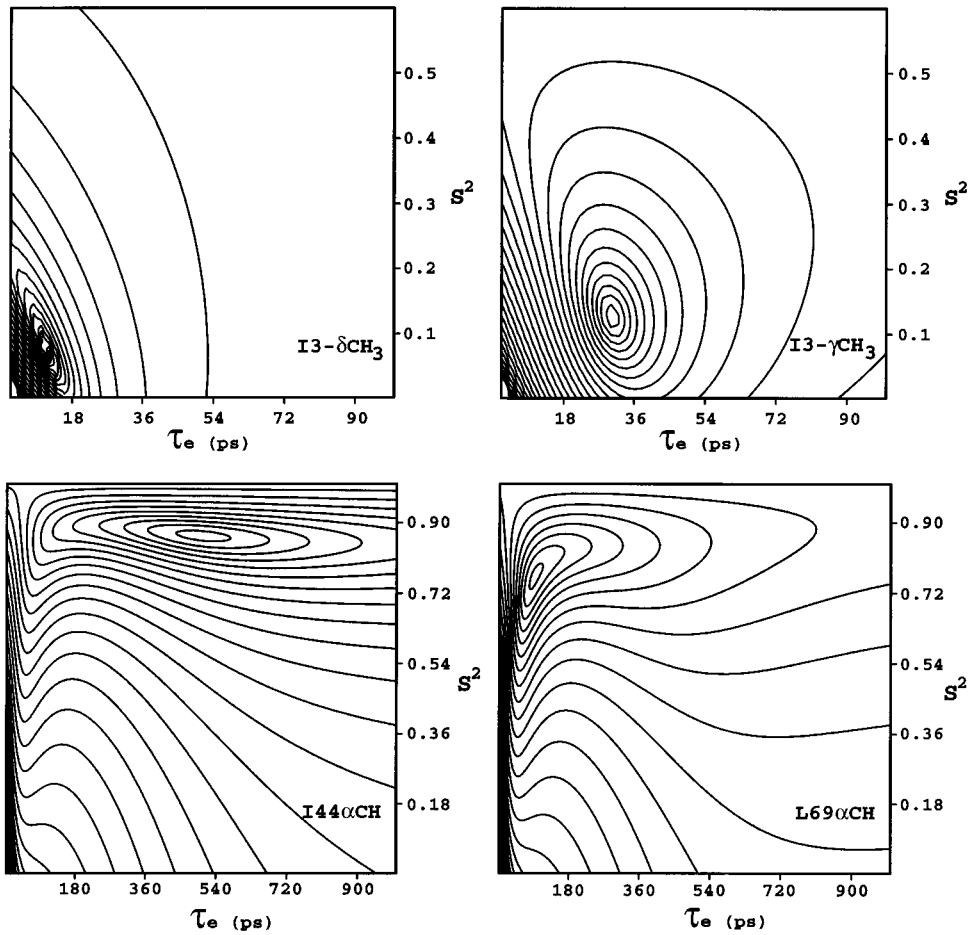

FIGURE 5: Examples of the behavior of the error function defined by eq 4 in determining local model free parameters. Shown are contours of the error function determined by sampling reasonable ranges of values for S^2 and τ_e. Examples are shown for the methyl carbons of Ile-3 and the α carbons of Ile-44 and Leu-69.

rapid axially symmetric motion of a purely tetrahedral methyl group. Order parameters larger than 0.111 could in principle be due to contributions arising from nontetrahedral geometry, restricted motion due, for example, to steric hindrance, non-dipolar relaxation mechanisms including cross-correlation effects, or inaccurate relaxation parameters. As pointed out above, non-dipolar relaxation mechanisms such as spin rotation or chemical shift anisotropy can be confidently excluded for methyl group relaxation. The experimental design employed also makes cross-correlation effects unlikely, as is evidenced by the decidedly single exponential character of the obtained spin lattice relaxation curves (see Figure 3 and Wand et al., 1995). The data used to determine the reported model free parameters are of uniform quality with nothing distinguishing sites with order parameters exceeding the Woessner limit from those that do not. This leaves deviation from fast three site or continuous diffusion motion for the methyl group, perhaps due to steric restriction, or distortion of the methyl group geometry as potential origins for the unusually high order parameters obtained at a small number of sites. There is precedence for the former (e.g., Dellwo & Wand, 1989) and for the latter (see below). When S^2 is much less than 0.111, it is likely that additional motion of the symmetry axis is further reducing the generalized order parameter. It is the motion of the methyl group symmetry axis which is of most interest here. The generalized order parameter for the symmetry axis, S^2_{axis}, can be obtained by simply dividing the obtained generalized order parameter by the Woessner value of 0.111.

As discussed in some detail by Nicholson et al. (1992), the sensitivity of S^2 to the geometry of the methyl group is potentially the limiting factor in the determination of S^2_{axis}. Single neutron diffraction studies of L-alanine (Lehmann et al., 1972) and L-valine (Koetzle et al., 1974) indicate that the methyl group may be distorted from pure tetrahedral geometry, presenting a potential uncertainity of perhaps up to 20% in obtained S^2_{axis} values.

The generalized order parameters obtained for 45 methyl groups of human ubiquitin are shown in Figure 7 and Table 2. Monte Carlo estimates of the reliability of the obtained generalized order parameters indicate an average confidence interval of 0.036, which is small on the full scale of the order parameter (zero to one) but is relatively large on the Woessner scaled generalized order parameter for the methyl group symmetry axis (zero to 0.111). The γ methyls of Thr and the β methyls of Ala show generalized order parameters ranging from the Woessner limit to below 0.01, corresponding to S^2_{axis} values of 1 to less than 0.1. The eight residues having single methyl groups that could be quantitated are found in β sheet structure, α helical structure, and turns. Generalized order parameters for all 14 methyl groups of the seven isoleucine residues of ubiquitin were also determined (Figure 7). With one exception, Ile-23, the generalized order parameters of the γ methyls were equal to or greater than those of the corresponding δ methyls, indicating higher mobility away from the main chain. It should be noted that many of these Ile side chains are completely buried and that the increased mobility away from the main chain

Table 1: α Carbon Relaxation Parameters Obtained for Randomly Fractionally ^{13}C-Enriched Recombinant Human Ubiquitin[a]

residue	NOE (125 MHz)	T_1 (s) (125 MHz)	T_1 (s) (186 MHz)	χ^2 ($\times 10^3$)	S^2	τ_e(ns)
M1	1.38	0.36	0.75	1.36	0.85	0.41
Q2	1.28	0.33	0.85	6.13	0.90	≥1.00
V5	1.15[b]	0.42	0.89	0.09	0.99	≤0.01
K6	1.37	0.41	0.77	0.16	0.86	0.18
T7	1.20	0.38	0.77	0.01	0.91	≥1.00
T9	1.29	0.44	0.71	3.21	0.88	0.38
K11	1.96	0.24	0.74	62.00	0.38	0.44
$T_1$2	1.43	0.39	0.71	0.07	0.83	0.26
I13	1.05[b]	0.39	0.69	2.51	0.88	≥1.00
$T_1$4	1.43	0.40	0.76	≤0.01	0.84	0.18
L15	nd[c]	0.32	0.70	≤0.01	0.50	0.36
E16	nd	0.37	0.77	0.18	0.91	≥1.00
V17	nd	0.35	0.68	0.03	0.83	≥1.00
E18	1.59	0.39	0.81	2.38	0.78	0.14
P19	1.57	0.40	0.83	1.92	0.77	0.12
T22	1.05[b]	0.38	0.88	1.50	0.98	≥1.00
I23	1.43	0.37	0.95	7.45	0.91	0.17
E24	2.10	0.52	0.82	1.23	0.38	0.08
V26	1.56	0.45	1.07	8.01	0.73	0.05
K27	1.04	0.36	0.63	3.34	0.82	≥1.00
A28	1.18	0.42	0.89	≤0.01	0.99	0.09
I30	1.19	0.39	0.78	≤0.01	0.93	≥1.00
Q31	1.46	0.33	0.80	8.76	0.83	0.39
K33	1.26	0.35	0.71	0.22	0.85	0.98
E34	0.98[b]	0.24	0.73	39.20	0.65	≥1.00
I36	1.27	0.39	1.01	5.60	0.98	≤0.01
P37	1.38	0.28	0.66	7.33	0.69	31.00
P38	1.64	0.30	0.90	26.90	0.78	0.33
D39	1.93	0.41	0.74	2.05	0.56	0.12
Q40	1.51	0.33	0.84	9.04	0.84	0.30
Q41	1.14	0.33	0.77	2.79	0.88	≥1.00
R42	1.62	0.23	0.78	63.00	0.48	≥1.00
L43	1.29	0.41	0.67	1.32	0.85	0.55
I44	1.31	0.42	0.70	1.77	0.87	0.38
A46	1.41	0.43	0.79	0.07	0.81	0.11
K48	1.18	0.38	0.73	0.18	0.90	≥1.00
L50	1.56	0.36	0.86	6.96	0.84	0.19
D52	2.28	0.28	0.81	47.09	0.49	0.26
R54	nd	0.33	0.51	≤0.01	0.50	0.36
T55	1.25	0.37	0.74	≤0.01	0.88	0.76
L56	1.39	0.41	0.81	0.23	0.87	0.15
S57	1.58	0.43	0.75	0.03	0.73	0.12
N60	1.32	0.40	0.89	1.13	0.92	0.11
I61	1.30	0.37	0.62	0.35	0.79	0.71
Q62	1.57	0.41	0.68	0.49	0.73	0.17
K63	1.51	0.41	0.82	1.00	0.81	0.13
E64	1.34	0.41	0.77	0.27	0.88	0.20
S65	1.09[b]	0.30	0.70	4.98	0.80	≥1.00
T66	1.33	0.35	0.69	0.24	0.83	0.59
L67	nd	0.33	0.73	2.77	0.84	≥1.00
L69	1.49	0.37	0.87	5.57	0.87	0.21
V70	1.75	0.38	0.76	3.98	0.71	0.17
L71	nd	0.36	0.67	≤0.01	0.80	0.47
R72	1.50	0.30	0.62	4.68	0.66	0.58
L73	1.93	0.31	0.53	1.08	0.45	0.30
R74	1.60	0.33	0.52	0.02	0.57	0.45

[a] Relaxation data obtained on 4 mM 15% randomly ^{13}C-enriched ubiquitin at 30 C in 50 mM sodium acetate buffer, pH* 5. Effective correlation times quoted at ≥1 ns are sufficiently close to the global tumbling time (4.125 ns) to violate a fundamental premise of the model free treatment. Order parameters and effective correlation times at these sites must be interpreted with caution. The goodness of fit (χ^2) at each site is defined by eq 5. The average 95% confidence interval for the obtained generalized order parameters is ±0.033. [b] Observed heteronuclear NOE is less than minimum predicted for a rigid ^{13}C−^{1}H bond vector isotropically tumbling with a correlation time of 4.125 ns. [c] nd, not determined.

arises from dynamics within a completely packed environment. Generalized order parameters for 16 methyl groups of nine leucines were also determined. Only one methyl,

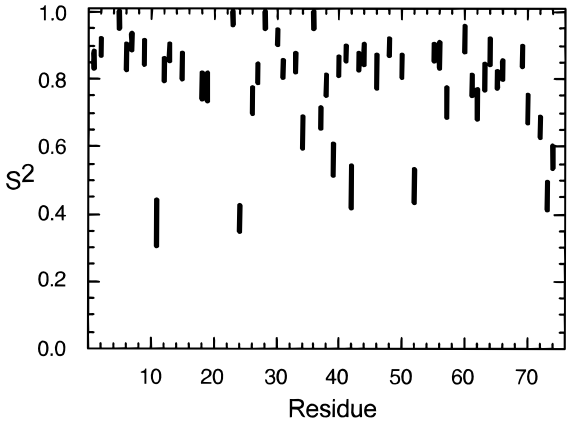

FIGURE 6: Determined generalized order parameters of α C−H vectors of human ubiquitin. The length of the vertical bar denotes the estimated 99% confidence limits of the given S^2 value as determined by Monte Carlo sampling. The contribution of chemical shift anisotropy to the observed relaxation was assumed to be zero.

the *pro-R* methyl of Leu-15, shows a generalized order parameter significantly above the Woessner limit. The rest are at or below the Woessner limit and range as low as 0.03. In six of the seven cases where the generalized order parameters of both prochiral methyl groups were determined, the *pro-R* methyl consistently shows a higher value than the *pro-S* methyl group (Figure 7). Generalized order parameters for seven methyl groups of four valines were also determined. The *pro-R* methyl group of Val-26 shows a generalized order parameter signficantly greater than the Woessner limit. There is no apparent correlation with prochirality and the relative value of the *pro-R* and *pro-S* methyl group generalized order parameters. It is interesting to note that the neutron diffraction studies cited above indicate that the two methyl groups have different covalent geometry, although it should be noted that Nicholson et al. (1992) predict that both methyl group geometries would give S^2 values less than the Woessner limit. The one case of significant violation of the Woessner limit suggests that steric hindrance to free rotation may be the origin of this behavior. This effect has been seen previously in cyclosporin A (Dellwo & Wand, 1989).

Geometric Interpretation of Methyl Symmetry Axis Motion. When reasonable values for S^2_{axis} can be obtained (i.e., $0 < S^2_{axis} < 1$; $0 < S^2 < 0.111$), then further physical insight into the generalized order parameter can often be derived from its interpretation within the context of a specific motional model. Two plausible models for the motion of the symmetry axis of a methyl group include the "diffusion in a cone" and "restricted diffusion" models. If the symmetry axis diffuses in a cone of semiangle θ, then the obtained S^2_{axis} determines θ by (Lipari & Szabo, 1982b)

$$\theta = \cos^{-1}\left[\frac{1}{2}((1 + 8S_{axis})^{1/2} - 1)\right] \qquad (6)$$

The generalized order parameters obtained for the symmetry axes of methyl groups of alanine and threonine correspond to cone angles ranging from effectively zero (e.g., Ala-46, Thr-9, Thr-12, Thr-55) to about 50° (e.g., Thr-7) and even close to 90° (Ala-28). The value obtained for Ala-46 is particularly interesting as it corresponds well with the generalized order parameter obtained for the α C−H vector to which the methyl symmetry axis is rigidly attached. The

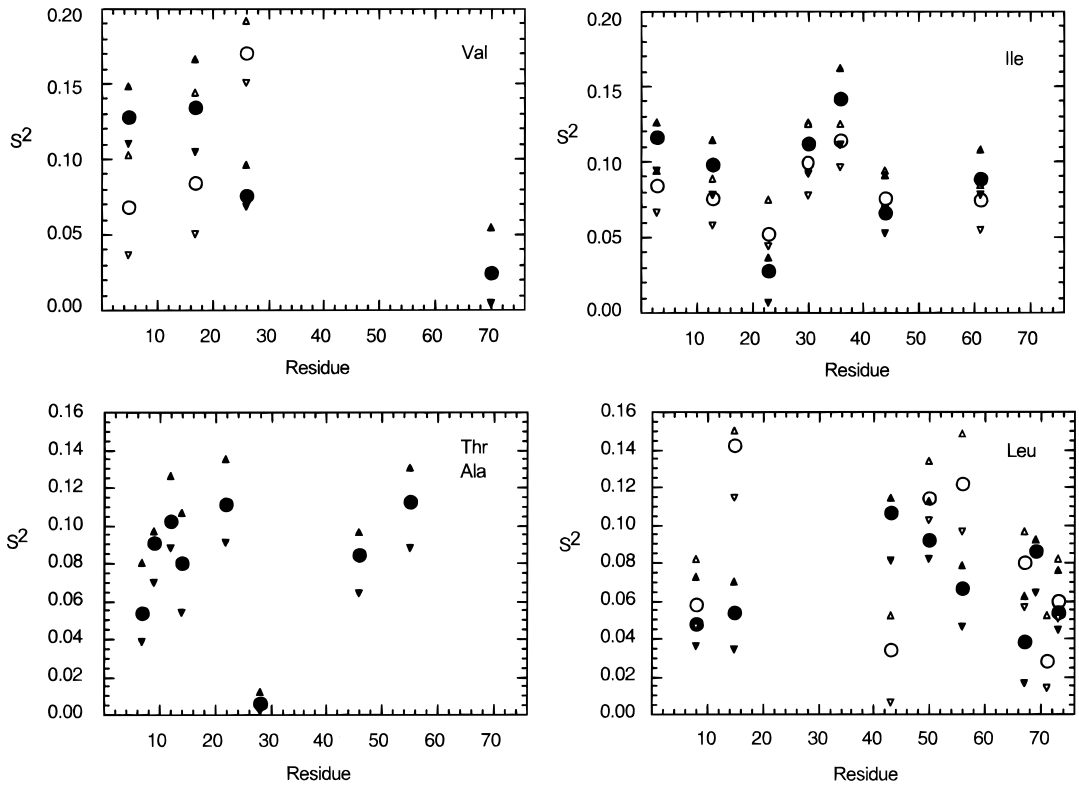

FIGURE 7: Determined generalized order parameters of methyl group C−H vectors of human ubiquitin. The upper left panel shows the S^2 values obtained for valine γ *pro-R* (open symbols) and γ *pro-S* (closed symbols) methyl groups. The upper right panel shows the S^2 values obtained for isoleucine γ (closed symbols) and δ (closed symbols) methyl groups. The lower left panel shows S^2 values obtained for threonine and alanine residues. The lower right panel shows S^2 values obtained for leucine δ *pro-R* (open symbols) and δ *pro-S* (closed symbols) methyl groups. Circles correspond to the value of S^2 at which the best fit to the relaxation data is obtained. The upward facing triangles and lower facing triangles denote the estimated 99% confidence limits of the given S^2 value as determined by Monte Carlo sampling. The contribution of chemical shift anisotropy to the observed relaxation was assumed to be zero.

equivalence of generalized order parameters suggests that the director axis of the motion dominating relaxation bisects the $C_\alpha-H$ and $C_\alpha-C_\beta$ bond vectors. In contrast, the director axis of the motion dominating relaxation at Ala-28 must be at quite different angles to the $C_\alpha-H$ and $C_\alpha-C_\beta$ bond vectors. The effective correlation times for the Thr methyl groups average 27 ± 5 ps. The obtained S^2_{axis} values for six δ methyl groups of the isoleucine residues correspond to an average cone angle of 31 ± 4°. The effective correlation times for these six δ methyl groups average 13 ± 4 ps.

To extend this type of analysis to the methyl pairs of valine and leucine, one could imagine that the symmetry axis of a methyl group moves by virtue of its rigid attachment to a director rotation axis. An example would be the rotation of the methyl symmetry axes of the γ methyls of valine about the director axis defined by the $C_\alpha-C_\beta$ bond. The director axis is at a fixed angle b to the methyl symmetry axis. If rotation about the director is restricted within some angular range $\pm\gamma$, then the order parameter for the axis is given by (Lipari & Szabo, 1982b):

$$S^2_{axis} = (P_2(\cos\beta))^2 + \frac{3\sin^2\beta\sin^2\gamma}{\gamma^2}\left(\cos^2\beta + \frac{1}{4}\sin^2\beta\cos^2\gamma\right) \quad (7)$$

where β is the angle between the symmetry axis and the director axis and is 70.5° in this case, and γ is the restriction angle. The restricted diffusion model also predicts that the S^2_{axis} parameters for each methyl pair of valine and leucine should be the same. Different values indicate that the effective director axis does not simply coincide with the carbon−carbon bond. As one of the methyl groups of each of the three valine residues has an S^2_{axis} parameter exceeding the Woessner limit, these side chains should not be considered in the context of this model. For the most of the leucine residues, for which S^2_{axis} parameters for both methyl groups could be obtained, the S^2_{axis} parameters are sufficiently different to suggest the presence of more complicated motions. It should be noted that a recent study employing deuterium relaxation in partially deuterated methyl groups of the C-terminal SH2 domain from phospholipase $C\gamma_1$ while showing the same overall range of S^2_{axis} parameter values did not show such large differences between prochiral methyl groups of the same side chain (Muhandiram et al., 1995). The effective correlation times for each methyl pair of valine and leucine residues are generally quite similar and cluster between 10 and 50 ps.

CONCLUDING REMARKS

These studies have employed a simple, recently introduced approach to obtain reliable ^{13}C-relaxation parameters of methine and methyl carbons at an unprecedented number of sites within a protein. The data obtained using recombinant human ubiquitin have been analyzed in the context of the Lipari−Szabo "model free" formalism. The main chain α C−H vectors behave in a manner analagous to the highly restricted motion seen in previous studies of the motion of amide N−H vectors (Schneider et al., 1992). In distinct

Table 2: Methyl Carbon Relaxation Parameters Obtained for Randomly Fractionally ^{13}C-Enriched Recombinant Human Ubiquitin[a]

residue	methyl	NOE (125 MHz)	T_1 (s) (125 MHz)	T_1 (s) (186 MHz)	χ^2 ($\times 10^3$)	S^2	τ_e (ps)
I3	γ	2.23	0.46	0.49	3.26	0.12	28
I3	δ	1.88	1.02	1.23	4.28	0.08	8.1
V5	γR	nd[b]	0.51	0.60	0.02	0.07	26
V5	γS	1.83	0.69	0.77	5.37	0.13	14
T7	γ	2.60	0.45	0.48	0.08	0.05	34
L8	δR	2.53	0.53	0.60	0.02	0.06	26
L8	δS	2.61	0.54	0.62	0.15	0.05	26
T9	γ	2.29	0.55	0.62	1.38	0.09	22
$T_1$2	γ	2.32	0.46	0.55	0.06	0.10	28
I13	γ	2.20	0.56	0.61	2.32	0.10	22
I13	δ	2.16	0.79	0.90	1.53	0.08	14
$T_1$4	γ	2.52	0.42	0.48	0.02	0.08	34
L15	δR	1.99	0.52	0.55	6.63	0.14	22
L15	δS	2.50	0.63	0.67	0.56	0.05	22
V17	γR	nd	0.45	0.53	$\leq$0.01	0.08	30
V17	γS	2.39	0.30	0.35	0.47	0.13	48
T22	γ	2.19	0.49	0.59	0.61	0.11	24
I23	γ	2.92	0.55	0.65	0.67	0.03	26
I23	δ	2.42	0.68	0.75	0.41	0.05	20
V26	γR	1.93	0.45	0.58	1.08	0.17	22
V26	γS	2.27	0.69	0.87	0.01	0.08	16
A28	β	2.17	1.55	1.51	1.71	0.01	10
I30	γ	2.21	0.53	0.67	0.22	0.11	20
I30	δ	1.89	0.91	1.01	7.89	0.10	10
I36	γ	2.55	0.29	0.39	1.26	0.14	46
I36	δ	1.71	0.91	1.09	6.89	0.11	8.1
L43	δR	2.92	0.40	0.47	0.98	0.03	38
L43	δS	2.22	0.56	0.67	0.91	0.11	20
I44	γ	2.52	0.49	0.57	0.02	0.07	28
I44	δ	2.01	0.88	1.05	1.00	0.08	12
A46	β	2.20	0.71	0.79	2.22	0.08	16
L50	δR	2.11	0.55	0.66	0.80	0.11	20
L50	δS	1.95	0.77	0.88	2.63	0.09	14
T55	γ	2.28	0.45	0.51	1.06	0.11	28
L56	δR	2.45	0.35	0.46	0.30	0.12	36
L56	δS	2.35	0.69	0.77	1.28	0.07	18
I61	γ	2.15	0.66	0.74	1.20	0.09	18
I61	δ	2.18	0.80	0.90	1.93	0.07	14
L67	δR	2.51	0.43	0.48	0.34	0.08	32
L67	δS	2.59	0.53	0.52	1.78	0.04	30
L69	δS	2.32	0.57	0.62	2.00	0.09	22
V70	γS	2.89	0.36	0.41	0.33	0.02	44
L71	δR	2.74	0.49	0.53	0.08	0.03	32
L73	δR	2.49	0.57	0.64	0.03	0.06	24
L73	δS	2.45	0.63	0.71	0.16	0.05	22

[a] Relaxation data obtained on 4 mM 15% randomly ^{13}C-enriched ubiquitin at 30 C in 50 mM sodium acetate buffer, pH* 5. Effective correlation times quoted at $\geq$1 ns are sufficiently close to the global tumbling time (4.125 ns) to violate a fundamental premise of the model free treatment. Order parameters and effective correlation times at these sites must be interpreted with caution. The goodness of fit (χ^2) at each site is defined by eq 5. The average 95% confidence interval for the obtained generalized order parameters is $\pm$0.018. [b] nd, not determined.

contrast, the analysis presented here indicates an unexpected *range* of dynamics within the interior of the protein. This has several implications. First and perhaps foremost is the suggestion that the interior of the protein is not only dynamic but heterogeneously so. The presence of potentially spatially extensive dynamics within the core of the protein points to the existence of considerable side chain entropy. Side chain conformational entropy is one of many components of the free energy balance that leads to the marginal stability of proteins. The changes in side chain conformational entropy upon folding have been estimated on the basis of (presumed) conformationally restricted models for the native state and various degrees of conformational freedom for the unfolded state to range between 0 and -2 kcal mol^{-1} at 300 K, depending on amino acid type (for a recent review, see Doig & Sternberg, 1995). This implies that many interior side chains are potentially interconverting between discrete states (i.e., barrier crossing) and/or moving within potential wells which are broader than usually imagined. In either case, the residual side chain entropy is potentially significant. Second, the data presented here suggest that the conformational entropy changes experienced by burial of a side chain are context dependent and may not be estimated on the basis of amino acid type alone. Thus, although somewhat qualitative, these arguments promote the need to expand the view of the side chain dynamics of proteins by extension to the motions of methylene centers and to ultimately quantitatively relate the internal dynamics to residual conformational entropy. Such studies are in progress and will be reported elsewhere.

ACKNOWLEDGMENT

We thank Professor Gregorio Weber for helpful discussion and Dr. Ad Bax for helpful comments and communicating results prior to publication. We are indebted to Dr. Milo Westler for assistance collecting data at the National NMR Facility at Madison. We also thank Dr. Peter Domaille for communicating preliminary results prior to publication.

SUPPORTING INFORMATION AVAILABLE

One table of ^{1}H, ^{13}C, and ^{15}N resonance chemical shift assignments; one figure documenting leucine and valine prochiral methyl assignments (8 pages). Ordering information is given on any current masthead page.

REFERENCES

Bax, A., Clore, M., & Gronenborn, A. M. (1990) *J. Magn. Reson. 88*, 425−431.

Clore, G. M., Szabo, A., Bax, A., Kay, L. E., Driscoll, P. C., & Gronenborn, A. M. (1991) *J. Am. Chem. Soc. 112*, 4989−4991.

Dellwo, M. J., & Wand, A. J. (1989) *J. Am. Chem. Soc. 111*, 4571−4578.

Dellwo, M. J., & Wand, A. J. (1991) *J. Magn. Reson. 91*, 505−516.

Di Stefano, D. L., & Wand, A. J. (1987) *Biochemistry 28*, 7272−7281.

Doig, A. J., & Sternberg, M. J. E. (1995) *Protein Science 4*, 2247−2251.

Ecker, D. J., Butt, T. R., Marsh, J., Sternberg, E. J., Margolis, N., Monia, B. P., Jonnalagadda, S., Khan, M. I., Weber, P. L., Mueller, L., & Crooke, S. T. (1987a) *J. Biol. Chem. 262*, 14213−14221.

Ecker, D. J., Khan, M. I., Marsh, J., Butt, T. R., & Crooke, S. T. (1987b) *J. Biol. Chem. 262*, 3524−3527.

Grzesiek, S., & Bax, A. (1992) *J. Magn. Reson. 96*, 432−440.

Karplus, M., Ichiye, T., & Petitt, B. M. (1987) *Biophys. J. 52*, 1083−1085.

Kay, L. E., & Torchia, D. A. (1991) *J. Magn. Reson. 95*, 536−547.

Kay, L. E., Bull, T. E., Nicholoson, L. K., Griesinger, C., Schwalbe, H., Bax, A., & Torchia, D. A. (1992) *J. Magn. Reson. 100*, 538−558.

Koetzle, T. F., Golic, L., Lehmann, M. S., Verbist, J. J., & Hamilton, W. C. (1974) *J. Chem. Phys. 60*, 4690−4696.

Lehmann, M. S., Koetzle, T. F., & Hamilton, W. C. (1972) *J. Am. Chem. Soc. 94*, 2657−2660.

Lipari, G., & Szabo, A. (1982a) *J. Am. Chem. Soc. 104*, 4546−4559.

Lipari, G., & Szabo, A. (1982b) *J. Am. Chem. Soc. 104*, 4559−4570.

Muhandiram, D. R., Yamazaki, T., Sykes, B. D., & Kay, L. E. (1995) *J. Am. Chem. Soc. 117*, 11536−11544.

Neri, D., Szyperski, T., Otting, G., Senn, H., & Wüthrich, K. (1989) *Biochemistry 28*, 7510−7516.
Neri, D., Otting, G., & Wüthrich, K. (1990) *Tetrahedron 46*, 3287−3296.
Nicholson, L. K., Kay, L. E., Baldisseri, D. M., Arango, J., Young, P. E., Bax, A. & Torchia, D. A. (1992) *Biochemistry 31*, 5253−5263.
Palmer, A. G., III, Wright, P. E., & Rance, M. R. (1991) *Chem. Phys. Lett. 185*, 41−46.
Sambrook, J., Fritsch, E. F., & Maniatas, T. (1989) *Molecular Cloning*, 2nd ed., Cold Spring Harbor Laboratory Press, Cold Spring Harbor, NY.
Sklenar, V., Torchia, D., & Bax, A. (1987) *J. Magn. Reson. 73*, 375−379.
Spiess, H. W. (1978) *NMR: Basic Princ. Prog. 15*, 55−214.
Spiess, H. W., Schweitzer, D., & Haeberlen, U. (1973) *J. Magn. Reson. 9*, 444−460.
Tjandra, N., Feller, S. E., Pastor, R. W., & Bax, A. (1996) *J. Am. Chem. Soc. 117*, 12562−12566.
Vuister, G., & Bax, A. (1992) *J. Magn. Reson. 98*, 428−435.
Wand, A. J., Bieber, R. J., Urbauer, J. L., McEvoy, R. P., & Gan, Z. (1995) *J. Magn. Reson. Ser. B*, 173−175.
Wang, A. C., Grzesiek, S., Tschudin, R., Lodi, P. J., & Bax, A. (1995) *J. Biomol. NMR 5*, 376−382.
Werbelow, L. G., & Grant, D. M. (1977) in *Advances in Magnetic Resonance* (Waugh, J. S., Ed.) Vol. 9, p 189, Academic Press, New York.
Wittebort, R. J., & Szabo, A. (1978) *J. Chem. Phys. 69*, 1722−1736.
Woessner, D. E. (1962) *J. Chem. Phys. 36*, 1−4.

BI9530144